Improved Wood Species Identification Based On Multi-View Imagery of The Three Anatomical Planes

Núbia Rosa Da Silva (✉ nubia@ufcat.edu.br)
  Ghent University   https://orcid.org/0000-0003-1982-5144

Victor Deklerck
  Royal Botanic Gardens Kew

Jan Baetens
  Ghent University

Jan Van den Bulcke
  Ghent University

Maaike De Ridder
  Royal Museum for Central Africa

Mélissa Rousseau
  Royal Museum for Central Africa

Odemir Martinez Bruno
  University of Sao Paulo Campus of Sao Carlos

Hans Beeckman
  Royal Museum for Central Africa

Joris Van Acker
  Ghent University

Bernard De Baets
  Ghent University

Jan Verwaeren
  Ghent University

Research Article

Improved wood species identification based on multi-view imagery of the three anatomical planes

Núbia Rosa da Silva* · **Victor Deklerck** ·
Jan M. Baetens · **Jan Van den Bulcke** ·
Maaike De Ridder · **Mélissa Rousseau** ·
Odemir Martinez Bruno · **Hans
Beeckman** · **Joris Van Acker** · **Bernard
De Baets** · **Jan Verwaeren**

Abstract
Background
The identification of tropical African wood species based on microscopic im-

Núbia Rosa da Silva
KERMIT, Department of Data Analysis and Mathematical Modelling, Ghent University, Ghent, Belgium
Institute of Mathematics and Computer Science, University of São Paulo, São Carlos, Brazil E-mail: *nubia@ufcat.edu.br, nubiasrosa@gmail.com
Present address: Federal University of Catalão, Catalão, Goiás, Brazil

Victor Deklerck
Royal Botanic Gardens Kew, Richmond, Surrey, United Kingdom

Jan M. Baetens
KERMIT, Department of Data Analysis and Mathematical Modelling, Ghent University, Ghent, Belgium

Jan Van den Bulcke
Laboratory of Wood Technology, Department of Environment, Ghent University, Ghent, Belgium

Maaike De Ridder
Service of Wood Biology, Royal Museum for Central Africa, Tervuren, Belgium

Mélissa Rousseau
Service of Wood Biology, Royal Museum for Central Africa, Tervuren, Belgium

Odemir Martinez Bruno
São Carlos Institute of Physics, University of São Paulo, São Carlos, Brazil
Institute of Mathematics and Computer Science, University of São Paulo, São Carlos, Brazil

Hans Beeckman
Service of Wood Biology, Royal Museum for Central Africa, Tervuren, Belgium

Joris Van Acker
Laboratory of Wood Technology, Department of Environment, Ghent University, Ghent, Belgium

Bernard De Baets
KERMIT, Department of Data Analysis and Mathematical Modelling, Ghent University, Ghent, Belgium

Jan Verwaeren
KERMIT, Department of Data Analysis and Mathematical Modelling, Ghent University, Ghent, Belgium

agery is a challenging problem due to the heterogeneous nature of the composition of wood combined with the vast number of candidate species. Image classification methods that rely on machine learning can facilitate this identification, provided that sufficient training material is available. Despite the fact that the three main anatomical sections contain information that is relevant for species identification, current methods only rely on the transversal section. Additionally, commonly used procedures for evaluating the performance of these methods neglect the fact that multiple images often originate from the same tree, leading to an overly optimistic estimate of the performance.

Results

We introduce a new image dataset containing microscopic images of the three main anatomical sections of 77 Congolese wood species. A dedicated multi-view image classification method is developed and obtains an accuracy (computed using the naive but common approach) of 95%, outperforming the single-view methods by a large margin. An in-depth analysis shows that naive accuracy estimates can lead to a dramatic over-prediction, of up to 60%, of the accuracy.

Conclusions

Additional images from the non-transversal sections can boost the performance of machine-learning-based wood species identification methods. Additionally, care should be taken when evaluating the performance of machine-learning-based wood species identification methods to avoid an overestimation of the performance.

Keywords wood species identification · wood anatomical cross-sections · texture analysis · machine vision · machine learning

1 Background

1.1 Illegal wood trade and wood species identification

Illegal logging is the most profitable natural resource crime and illegal wood accounts for 10 to 30 percent of the total global trade in wood products [1, 2], and increasing up to 50 and 90 percent when focusing on Southeast Asia, Central Africa, and South America [1]. The financial value of illegal logging is estimated at US$52 to 157 billion dollars per year. There also is a high risk of irreversible damage to ecosystems associated with the exploitation of highly sought after, sometimes protected, species. To prevent the over-exploitation of these species, protection measures are put in place, for example the Convention on International Trade in Endangered Species of Wild Fauna and Flora [3]. In addition, policy measures (for example EUTR and U.S. Lacey Act) are implemented in countries to counter the trade in illegal wood and to improve forest law enforcement and governance [4].

To enforce these regulations and policy measures, wood species identification techniques combined with robust datasets are needed. Wood species identification is currently mainly done via wood anatomical analysis and DART

TOFMS, proven to be successful in routine controls, and there are other viable techniques as well, for example DNA analysis and Near InfraRed spectroscopy [5–13]. Wood anatomical analysis is the most widely applied, readily available and least expensive technique. Identification is possible via an analysis of tissue and cell features through hand lenses, light or electronic microscopes or 2D or 3D scans and the IAWA list of microscopic features [14]. The IAWA characteristics are based on patterns of anatomical features, such as vessels, rays, parenchyma and fibres. The approach is usually sufficient to identify the genus, but sometimes fails to determine the species [15,16]. Moreover, it can be difficult to discern between closely related taxa.

1.2 Automated identification through wood anatomical images

Wood anatomical analysis is a complicated task that can take several years to master and will always involve expert knowledge. Driven by the success of automation of image recognition in other fields, several attempts have been made to automate wood species identification using computer vision models that use digital imagery of anatomical sections as input. The construction of these models is mostly handled as a pattern recognition task in which: (1) a representative dataset of labeled digital images is collected (the label is the species); (2) a feature extraction procedure is applied; and (3) a machine learning classification algorithm is trained to discriminate the species using the features. The approaches found in literature mostly differ by the choices that are made within each of these steps. We present an overview hereafter.

Martins et al. [17] used an image dataset that consisted of 112 species, a rather large number compared to other studies, including both hardwood and softwood species with a total of 2240 or approximately 20 images of microscopic transversal images per species. The authors experimented with different feature descriptors and concluded that Local Binary Patterns (LBP) as a feature (texture) descriptor combined with Support Vector Machines (SVMs) as a classification algorithm yields the best performance. They reported an accuracy of 86.0%. Filho et al. [18] composed an image dataset containing 41 Brazilian species with a total of 2942 macroscopic transversal images. They adopted a strategy where first the image is divided in sub-images which are then classified independently. A different feature extractor is applied to each sub-image, resulting in separate feature vectors. Subsequently, a SVM (a probabilistic variant is used) is trained on each feature vector. The class probabilities that are predicted by the individual SVMs are aggregated through a fusion rule to obtain a final prediction. For the 41 species they reached an accuracy of 97.77%. Rosa da Silva et al. [19] used a dataset containing 1221 microscopic images of 77 commercial wood species from the Democratic Republic of the Congo. They used Local Phase Quantization (LPQ) as a feature descriptor and linear discriminant analysis as a classifier, resulting in an accuracy of approximately 88% at species level. Ravindran et al. [20] composed a dataset containing 2303 macroscopic images of 10 species from the Meliaceae fam-

ily. They used (deep) convolutional neural networks (CNN) as a classifier. The convolutional layers serve as data-driven feature extractors, obviating the need for feature descriptors. They obtained an accuracy of 87.4%. Recently, Souza et al. [21] used LBP in the construction of an automated recognition system of Brazilian forest species. Forty six species were used in their analysis, with a total of 1901 macroscopic images. An automatic recognition system based on the concatenation of rotation-invariant LBP histograms and an SVM classifier obtained an F1-score of 97.67%. This approach requires a large reference dataset that captures all potential variability within a species [15]. However, thanks to historical wood collections, there are many curated wood anatomical slices available that can be used as a reference for the identification. Similarly, Ravindran et al. [22] used CNNs to identify 12 self-defined classes based on macroscopic imagery of transversal cross-sections of species that are common in the United States. Using a training dataset containing 3126 images, they obtained an accuracy of 97.7%. Along that line, Lens et al. [23] reported a similar accuracy (over 98% using CNN) on 2240 microscopic images of transversal cross-sections of 112 species.

The literature reviewed above illustrates that machine-vision-based wood species identification systems can, in some cases, reliably identify wood species. However, there is still room for improvement at several levels. First, the machine vision systems described in literature only use images of the transversal anatomical plane. The tangential and radial anatomical planes can also include information that is relevant for the species identification. For example, the height of the rays can be an important characteristic that can only be seen on tangential and radial planes. To this date, image datasets that contain imagery of the different anatomical planes are not generally available. To fill this gap, we introduce a new multi-view dataset. Secondly, we propose to use the taxonomy of the considered species to build a hierarchical classifier. For classifiers that output a probability distribution over the species, the Bayesian optimal decision criterion based on a hierarchical cost function can be used to encode this hierarchy into the identification problem. Third, in most research, cross-validation approaches are used to assess the performance of the developed systems. However, it is not always clear how cross-validation procedures are applied. Most publications mention that traditional k-fold (possibly stratified at the species level) is used. It is important to note that imagery datasets often result from a limited number of distinct trees. When these images are used in a traditional (random) k-fold cross-validation scheme, the performance can be overestimated.

This potential shortcoming is also explicitly mentioned in [23] as a source of potential underestimation of intra-species variability, where the authors state that they were unable to trace back images to individual samples using the dataset of [17]. In this work, we critically compare the performances obtained using a traditional k-fold approach with those obtained using a leave-k-tree-out approach. Therefore, the purpose of this paper is threefold. (1) We introduce a new image dataset that contains images of the three anatomical planes of 77 Congolese wood species and propose a multi-view random forest model

that can identify a specimen at the species level using images of the three anatomical planes. We compare the performance of this multi-view approach with the performance that is obtained when using only the transversal cross-section. (2) We incorporate information on the higher taxonomic level (genus and family) into the classification model by post-processing the probability estimates of random forest models. (3) We study the influence of using a leave-k-tree-out approach during cross-validation.

2 Results

2.1 Single-view versus multi-view classification

Performance of single-view classifiers. In this section, we discuss the advantages of multi-view classification approaches, a first batch of experiments was performed using single-view classifiers and several data augmentation techniques. From Table 1, it can be inferred that the transversal view is most informative for identifying the species. Moreover, data augmentation helps to boost the performance. It is clear that partitioning the original image into four parts leads to an increase of the predictive performance from 0.56 to 0.75 where the size of the dataset is quadrupled replacing each 1000×1000 pixels image by four 500×500 pixels images.

Table 1: Accuracies obtained using single-view classifiers.

Data augmentation technique	Accuracy (± std)		
	Transversal	Tangential	Radial
500×500	0.75 (± 0.02)	0.69 (± 0.01)	0.54 (± 0.01)
500×500−OGRN	0.38 (± 0.02)	0.34 (± 0.01)	0.27 (± 0.01)
500×1000	0.71 (± 0.02)	0.71 (± 0.01)	0.52 (± 0.01)
1000×1000	0.56 (± 0.02)	0.42 (± 0.02)	0.42 (± 0.02)

Performance of multi-view classifiers. In a second batch of experiments, the added value of using a multi-view model was investigated. Table 2 shows the results of the MVRF model in terms of accuracy computed using 4-fold cross-validation. From these results, it is clear that the addition of LPQ features from additional anatomical planes leads to an improvement of the classification accuracy. The concatenation of features of the transversal plus tangential outperforms transversal features only by a large margin, whereas the addition of R only leads to minor improvements, possibly because the magnifications used have not been sufficient to extract relevant details. Moreover, the MVRF model shows a better performance as compared to the simple concatenation of LPQ features. This result shows that both the additional information that is available in the different cross-sections and the type of model

both contribute significantly to the performance. The best performance (0.95) is obtained using the MVRF model.

In Figure 1, the influence of extending the features derived from the transversal cross-section with those extracted from the tangential and radial cross-sections is visualized per species. It can be seen here that for the eleven species that exhibited the lowest accuracy, complementing the LPQ features of the transversal cross-section with features from the tangential and radial cross-sections improves the classification results significantly for all species (with the exception of a small decrease for *Afzelia bella*).
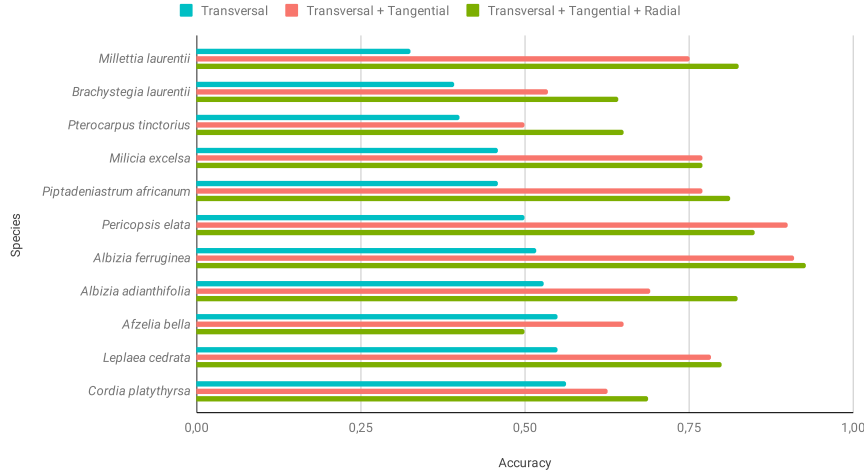

Fig. 1: Illustration of the influence of using only features from the transversal cross-sections and adding features from the tangential and radial cross-sections for the eleven species with the lowest accuracy (based on the transversal cross-section).

Gaining insight into the modes of failure. The results presented above illustrate that the overall accuracy of the classification model improves when features of additional cross-sections are added. Hereafter, we disentangle the reasons for this. Figures 2 (a)–(d) show score plots obtained after performing a principal component analysis (PCA) on the data matrix of the LPQ features (data of all 77 species). Figures 2 (a) and (c) show the score plot in the PCA space when only using transversal features and Figures 2 (b) and (d) show the score plot in the PCA space computed using the concatenated feature space transversal plus tangential. For the *Afzelia* species *Afzelia africana* and *Afzelia bipindensis* shown in Figures 2 (a) and 2 (b), it can be seen that in both cases, these species cannot easily be separated in the first two dimensions of the principal component space. This is as expected as both species cannot easily be distinguished by considering one or both cross-sections. On the other hand,

Table 2: Comparison of the results using the cross-sections separately and the random forest model. The first three columns respectively show the accuracy obtained using a random forest model trained on the LPQ features of the transversal images only (TV), a random forest model that uses the concatenation of LPQ features of the transversal and tangential cross-sections (TV+TG) and a random forest model that is obtained using the LPQ features from all three sections (TV+TG+R).

| | Accuracy (± std) | | | |
	TV	TV+TG	TV+TG+R	MVRF
500×500	0.75 (± 0.02)	0.86 (± 0.02)	0.89 (± 0.02)	**0.95 (± 0.01)**
500×500−OGRN	0.38 (± 0.02)	0.48 (± 0.02)	0.51 (± 0.02)	0.62 (± 0.03)
500×1000	0.71 (± 0.02)	0.85 (± 0.02)	0.87 (± 0.02)	0.91 (± 0.02)
1000×1000	0.56 (± 0.02)	0.62 (± 0.04)	0.66 (± 0.03)	0.66 (± 0.02)

Figures 2 (c) and 2 (d) show the score plots of *Entandrophragma candollei* and *Entandrophragma utile*. From these figures, it is clear that a better separation is observed when the LPQ features of the tangential cross-section are added. One of the main determinants to differentiate the two *Entandrophragma* species is seen only on the tangential plane. This explains that, when adding the features from the tangential cross-section, there is a better separation of the two *Entandrophragma* species. This is not the case for the *Afzelia* species, for which the tangential plane does not aid in the manual identification of these two species.

A more complete (and more quantitative) view on the improved separability due to the addition of information on the tangential cross-section is shown in Figures 3 and 4. Figure 3 shows the confusion matrix for the classification of all samples using only features of the transversal cross-section, while Figure 4 shows the confusion matrix for the classification using features of the transversal plus tangential cross-sections. Moreover, the phylogenetic tree is added to the left and top margins. It is clear that the highest values can be found at the diagonal and no other clear patterns can be discerned. From a phylogenetic point of view, no clear overall patterns can be observed in the confusion matrix. However, this confusion matrix illustrates that, for instance, within the *Afzelia* genus, there is quite some intra-genus confusion. A similar observation can be made for the *Cynometra* genus. The latter confusion matrix (Figure 4) is much cleaner, showing that the number of misclassifications decreases when adding features from the tangential cross-section. However, here as well the *Cynometra* genus has quite some inter-genus confusion.

2.2 Including genus and family information in the classification process

In a third batch of experiments, we investigated whether including information on the phylogeny into the learning process can improve the accuracy.
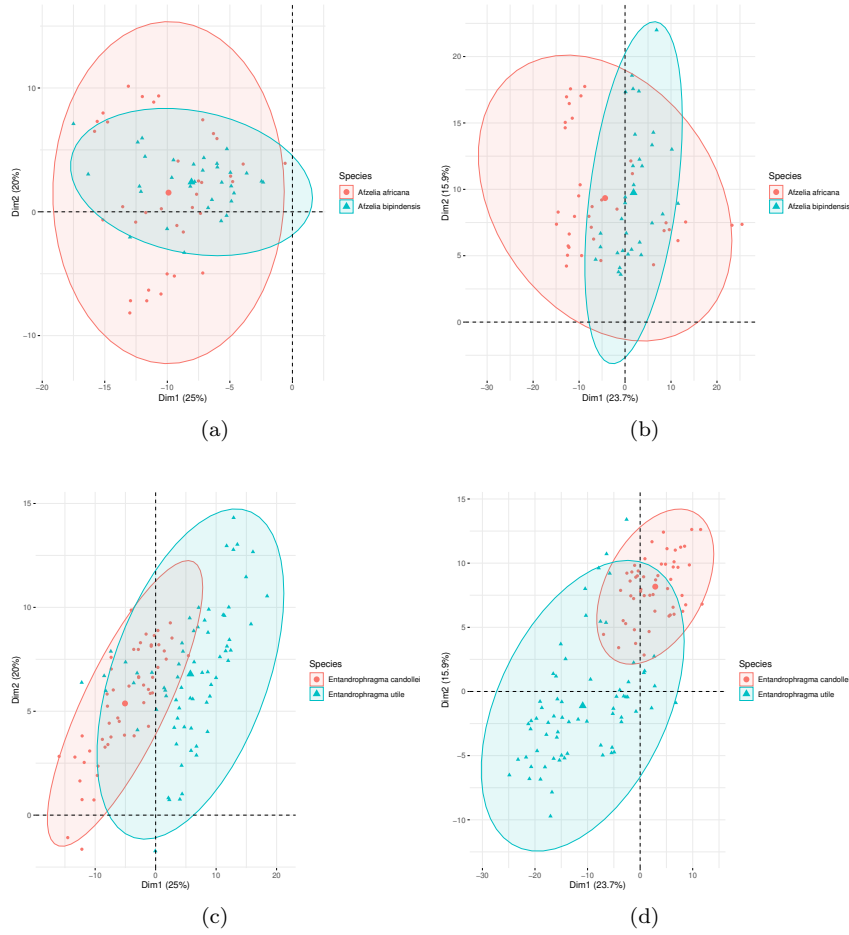
Fig. 2: 2D PCA-plot. Species *Afzelia africana* and *Afzelia bipindensis* using only features of the transversal cross-section (a) and adding features of the tangential cross-section (b). Species *Entandrophragma candollei* and *Entandrophragma utile* using only features of the transversal cross-section (c) and adding features of the tangential cross-section (d).

Table 3 shows the results that were obtained. The first column (RF) shows the accuracy obtained using the random forest classifier (1000×1000 pixels, so without data augmentation) trained using only the features derived from the transversal cross-section, using the species as a target. Moreover, this table also shows the accuracy of this same model at the genus and family level. The difference between these accuracies is rather small, implying that most of the classification errors already exist at the family level. Moreover, these results show that given a correct identification of the family, the probability that also
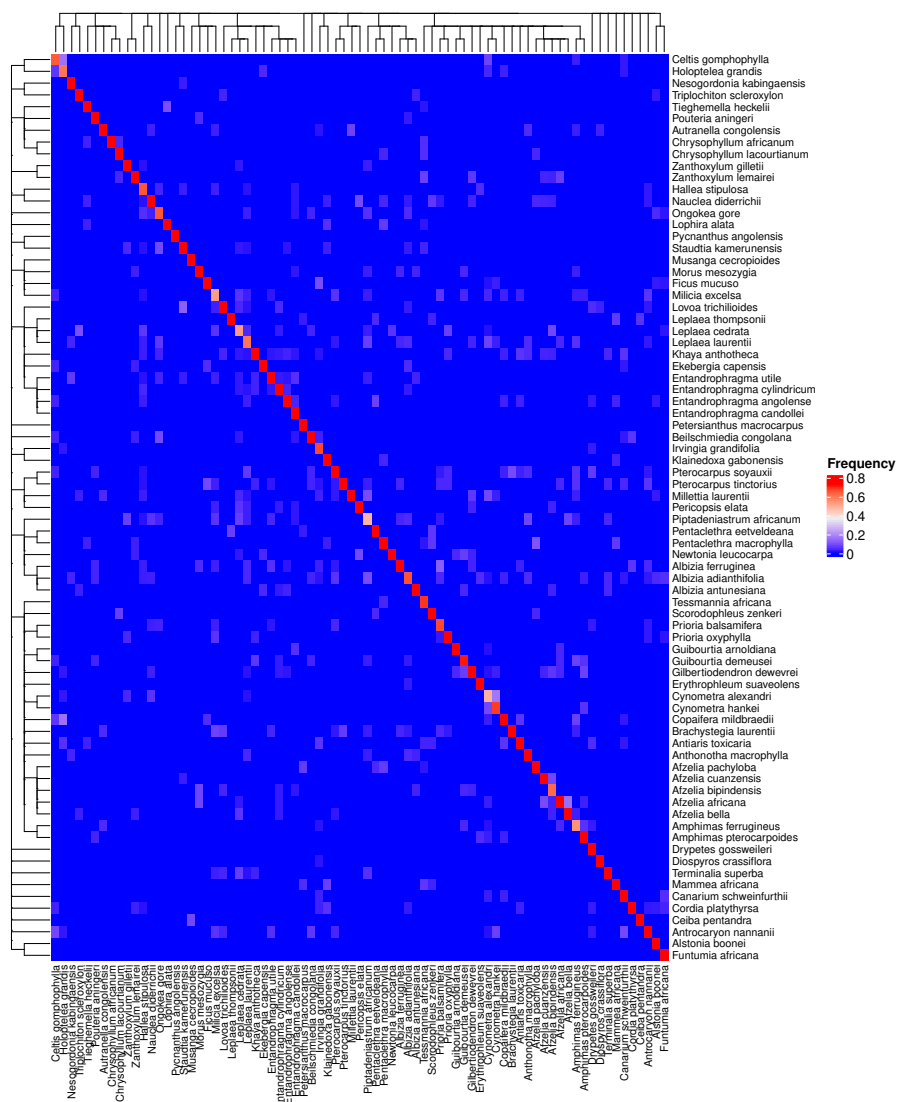
Fig. 3: Confusion matrix for the 500×500 dataset using features of the transversal cross-section.

the species will be identified correctly is 87.5%. The last row shows the average hierarchical loss H-Loss $= \frac{1}{n} \sum_{(y,\hat{y})} C(y,\hat{y})$ (which is minimized by the cost-sensitive algorithm), where the sum runs over all couples of observed labels y and predicted labels $\hat{y}$ and n is the number of test cases. This loss can be seen as a hierarchical combination of the losses observed at the species, genus and family levels (the range of this average loss is $[0; 1.5]$).
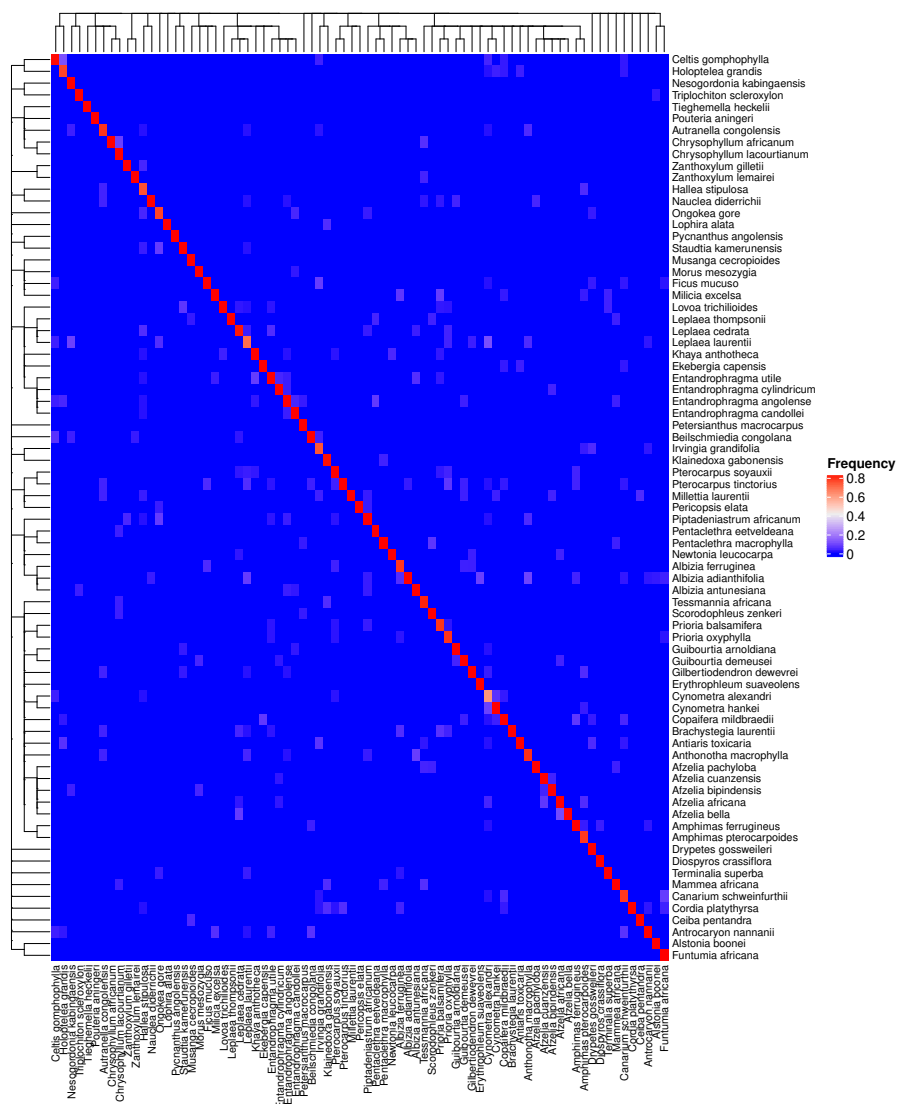
Fig. 4: Confusion matrix for the 500×500 dataset using features of the transversal plus tangential cross-section.

The second column shows the accuracies obtained using the cost-sensitive classification algorithm. From this table, it can be seen that the traditional random forest classifier consistently outperforms the cost-sensitive classifier. Even when using the H-Loss, the traditional random forest classifier outperforms its cost-sensitive version. From these results, we can conclude that this attempt to exploit the class hierarchy has a negative effect on the perfor-

mance. Nevertheless, this negative result provides some insight into the wood species identification problem. Most importantly, it shows that the posterior distribution, which is estimated by the random forest classifier, is not very informative, or is very poorly estimated. Even though the mode of the distribution is quite informative (as the accuracy of the traditional classifier at the species level is rather high), the estimates of probabilities for the remaining classes are not very useful and seem hard to exploit to gain predictive power. An explanation for this negative result, as well as a step towards a solution, can be found in recent literature on distribution free uncertain quantification or conformal prediction [24]. There, it is stated that there are no guarantees that the voting mechanism of the RF classifier leads to valid estimates of the class probabilities (in a frequentist sense). Conformal prediction approaches can be used to calibrate these probability estimates to produce confidence sets guaranteed to contain the ground truth with a user-specified probability. Even though these approaches are compatible with our approach, they require an additional (hold-out) dataset that is used in the calibration step. Unfortunately, the limited size of our dataset impedes the application of these approaches.

Table 3: Comparison of the accuracy of the random forest classifier (RF) with the cost-sensitive random forest classifier at different hierarchical levels using the transversal cross-section of the original dataset.

	RF	Cost-sensitive RF
Accuracy at species level	**0.56**	0.52
Accuracy at genus level	**0.58**	0.56
Accuracy at family level	**0.64**	0.63
H-Loss *(lower is better)*	**0.635**	0.683

2.3 Experiments using the leave-k-trees-out approach

In this last batch of experiments, for each species, all samples (images) from the same tree were separated for the test set, making the training set completely disjoint from the test set. In total, 165 samples from the original dataset were used for testing and 640 samples for training. When comparing the results of this leave-k-trees-out approach shown in Table 4 with the accuracy obtained using the traditional cross-validation schemes, we observe a dramatic decrease. This table clearly illustrates that the within tree variability is much smaller than the between-trees variability. It should be noted, however, that the number of observations per species was limited and therefore, reducing the training dataset to 165 samples will have an influence on the accuracy as well. Nevertheless, it remains striking that the performance deteriorates that strongly, which stresses the importance of performing this kind of cross-validation.

Table 4: Comparison of the accuracy of the leave-k-trees-out approach, where the test set is composed of images of trees that are not in the training set. The experiments were performed using the concatenation of the features of the three sections (TV+TG+R)) and the MVRF model.

	Accuracy ($\pm$ std)	
	TV+TG+R	MVRF
500×500	0.27 ($\pm$ 0.01)	0.23 ($\pm$ 0.01)
500×500−OGRN	0.22 ($\pm$ 0.01)	0.22 ($\pm$ 0.01)
500×1000	0.28 ($\pm$ 0.01)	0.25 ($\pm$ 0.01)
1000×1000	0.30 ($\pm$ 0.01)	0.28 ($\pm$ 0.01)

In our case, as the pieces of wood were obtained at different times and regions, there is large variability across the samples. Moreover, the small number of samples per species is an important reason for the low accuracy. Figure 10 in Supplementary Materials shows the selected samples for training and testing for the species *Lophira alata*, where we can see quite some variability between anatomical slices from the same species. This context reinforces the need for a representative dataset, with the availability of many samples and data augmentation operations.

3 Discussion

Identification analysis at the genus and family level is important because there are many similarities between species belonging to the same genus, which may, in some cases, explain misidentification. When using the multi-view random forest model, of the 14 errors in the samples of the genus *Afzelia*, five were predicted within the same genus. When considering the 10 misidentifications of samples of the genus *Cynometra*, six samples were identified as being of another species within the same genus. Considering the *Entandrophragma* genus, six erroneously identified samples were within the same genus. Of the four misidentifications of *Afzelia bella*, three were inside the same genus and from the three misidentifications of *Afzelia bipindensis*, all were in the same family and two were in the same genus.

Following this perspective, when examining the family level, the Fabaceae-Caesalpiniaceae family shows 62 misidentifications of samples at the species level, however, 19 of these are inside the own Fabaceae-Caesalpiniaceae family. In the Ulmaceae family, of the 12 misidentifications of samples at the species level, six misidentifications are inside the same family. The Meliaceae family shows 31 misidentifications of samples at the species level, with 17 misidentifications inside the Meliaceae family itself.

Exploring the Meliaceae family, out of the 10 species analyzed, three of them achieved an accuracy of one hundred percent: *Ekebergia capensis*, *Leplaea thompsonii* and *Lovoa trichilioides*. The average accuracy, considering the

10 analyzed species of the Meliaceae family, was 95% (species level). Within the *Entandrophragma* and *Khaya* genus, we can see several misidentifications. *Entandrophragma angolense*, *Entandrophragma candollei* and *Entandrophragma utile* are missclassified several times as *Khaya*. Two out of four misclassified samples from *Khaya anthotheca* were misclassified as *Entandrophragma*. Three out of six misclassified samples of *Leplaea cedrata* are misclassified as *Entandrophragma utile* and two out of four samples of *Entandrophragma utile* are misclassified as *Khaya anthotheca*.

Deklerck et al. [8] used metabolome profiles collected using Direct Analysis in Real Time (DART^{TM}) ionization coupled with Time-of-Flight Mass Spectrometry (DART-TOFMS) to analyze 95 specimens. A random forest model was used to perform the identification achieving an accuracy of 82.2%. They show that *Entandrophragma cylindricum* and *Entandrophragma utile* have different chemical fingerprints and they can separate the species using DART-TOFMS. In their work, *Khaya anthotheca* was sometimes misidentified as *Entandrophragma candollei* or *Entandrophragma angolense*, however was easily distinguished otherwise. In addition, the DART-TOFMS analysis was not able to accurately differentiate *Entandrophragma candollei* and *Entandrophragma angolense*.

In the work of Muellner et al. [25], six species of the Meliaceae family were identified using DNA barcoding reaching an accuracy of 67%. In Ravindran et al. [20], 10 species of the Meliaceae family were identified based on deep convolutional neural networks, achieving an accuracy of 87% at species the level and an accuracy of 96% at the genus level. Kitin et al. [26] used DART-TOFMS to study two species of *Afzelia*, *Afzelia pachyloba* and *Afzelia bipindensis*. Although the two species are not easily separated using the IAWA standard microscopic wood features, the results using DART-FORMS reached an accuracy of 78%.

Although there are different identification methods with acceptable accuracies, so far there is no method that is fully effective for identifying all wood species. Thus, one alternative is to use a combination of different methods, such as DART-FORMS, texture analysis and machine learning.

4 Conclusions

The images obtained to perform the experiments were extracted from wood samples collected at different time periods, which may have caused changes in texture features obtained from images of the same species. Weather conditions may affect the features of functional wood anatomy, such as vessel frequency and the development of the water transport pathways, making the pattern recognition task more complex.

The difficulty of obtaining wood samples is an important issue. In this way, being able to use different cross-sections from the same sample enriches the representativeness of each sample, improving the accuracy of the classification. However, just concatenating the features of the cross-sections is not enough,

as shown in the experiments. The need arises to create a model that is able to contemplate the features extracted from the different cross-sections. This way, this paper presented a random forest model that uses the out of bag probabilities provided by three types of texture images, being obtained from transversal, tangential and radial cross-section imagery. This approach showed better results than using a random forest model alone, even if the three sections are used in a concatenated way. The experiments showed that the results improved substantially when using the proposed model.

5 Method

5.1 Compilation of a multi-view image dataset

Datasets that contain imagery of the three anatomical sections of wood samples are not readily available. To fill this gap, we introduce a new image dataset containing images of the three anatomical planes of 77 Congolese species. Note that this dataset is an extension of the dataset used in [19].

The wood samples were collected in the Democratic Republic of the Congo. The wood anatomical slices were prepared by the Service of Wood Biology at the Royal Museum for Central Africa (Tervuren, Belgium). The cross-sections were cut with a sliding microtome, dehydrated in a graded ethanol series (50%, 75%, 96% and 100%) and fixed with Euparal. A light microscope (Olympus BX60) in connection with a digital camera (Olympus UC30) and the image analysis software package CellB (version 3.2, Olympus) were used for image acquisition. A standard magnification of $2.5\times$ the size of the sample was chosen for all pictures. All acquired images are RGB images of 1000×1000 pixels. In total, 805 wood slices belonging to 77 species, 58 genera and 25 families were used in this study (see Tables 5 and 6 in Supplementary Materials). Only slices with uniform texture, free of cracks and free of staining agents were chosen.

One wood slice generates three images, i.e., one image for each distinct cross sectional surface of the tree trunk: transversal, tangential and radial, as shown in Figure 5. The transversal anatomical section runs at right angles to the main axis of the stem or the trunk. The tangential cross-section cuts across the rays of a block of wood or a stem, while the radial cross-section runs parallel to the rays. All together, $805\times 3 = 2415$ images were obtained. Figure 6 shows samples from the three sections from five species of the genus Afzelia.

5.2 Data augmentation

On average only 10 images were available (for each species), which is too few for machine vision applications. Therefore, data augmentation was used to increase the number of samples per species. A first data augmentation step consisted of partitioning the original images (original size 1000×1000 pixels,
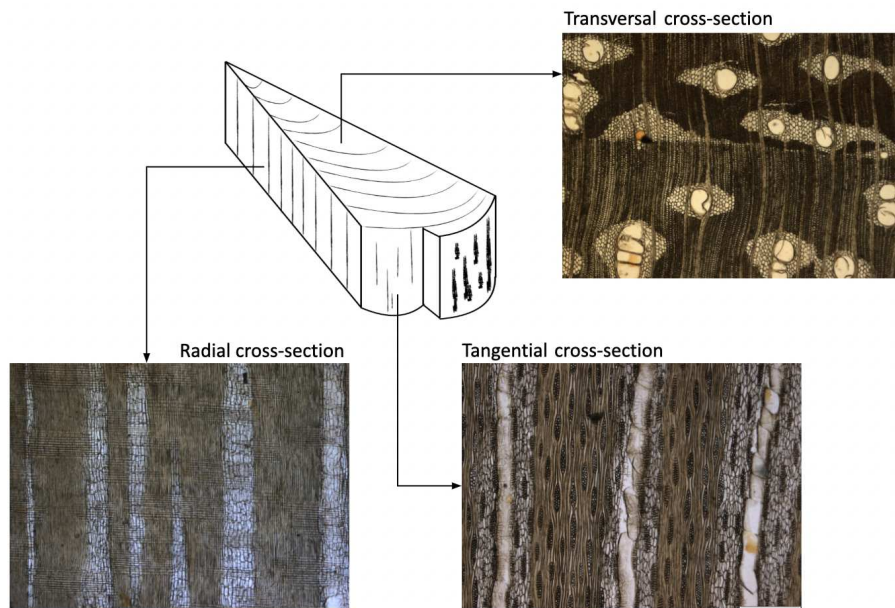
Fig. 5: Image acquisition of wood transversal, tangential and radial cross-sections of *Afzelia pachyloba*.

see Figure 7 (a)). Two options were explored: (1) dividing the original images in half (Figure 7 (b)), and (2) dividing the images into four parts, resulting in images of 500×500 pixels (Figure 7 (c)). In a second step, augmentation was performed by filtering using a 2-D Gaussian smoothing kernel with a standard deviation of 1, the creation of rotated versions by rotating the original images 90 degrees and the addition of salt-and-pepper noise with a density of 0.05 (Figure 7 (d)). All of these actions were performed on the three cross-sections. To be able to investigate the influence of this data augmentation step, we keep track of three datasets with images of different sizes: 1000×1000 pixels (original), 500×1000 pixels (partitioned by dividing in half), 500×500 pixels (partitioned by dividing into four parts) and 500×500−OGRN (partitioned into four parts, being the first piece, original – O, the second, smoothed – G, the third, rotated – R and the last one, noisy – N). The effect of the data augmentation step on the feature representation of the images (for the species *Afzelia africana*) is shown in Figure 9 in Supplementary Materials.
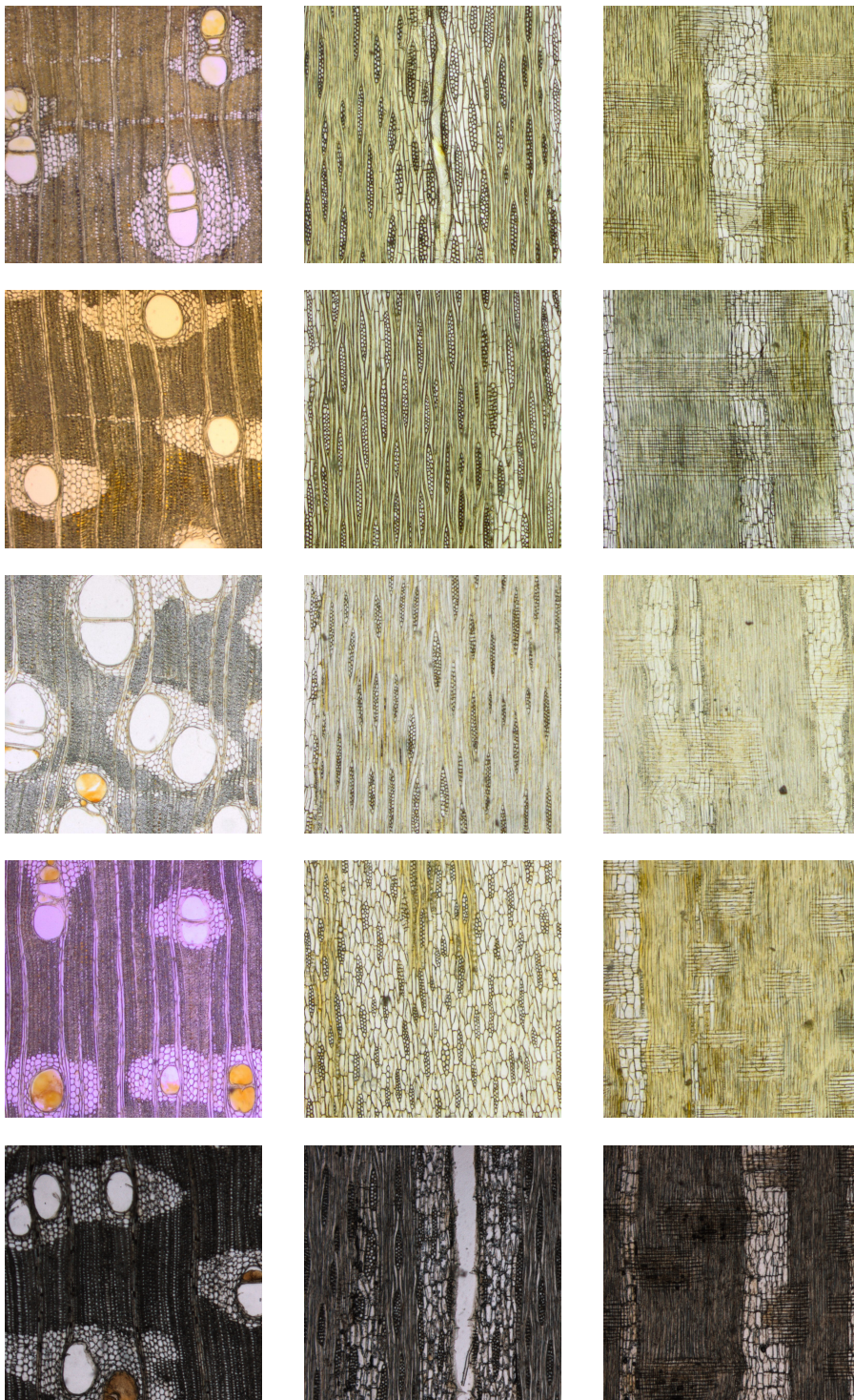
Fig. 6: Samples of the wood image dataset showing in each column: transversal, tangential and radial cross-sections. Each row shows a single species with the three planes, being, from top to bottom: *Afzelia africana*, *Afzelia bella*, *Afzelia bipindensis*, *Afzelia cuanzensis* and *Afzelia pachyloba*.
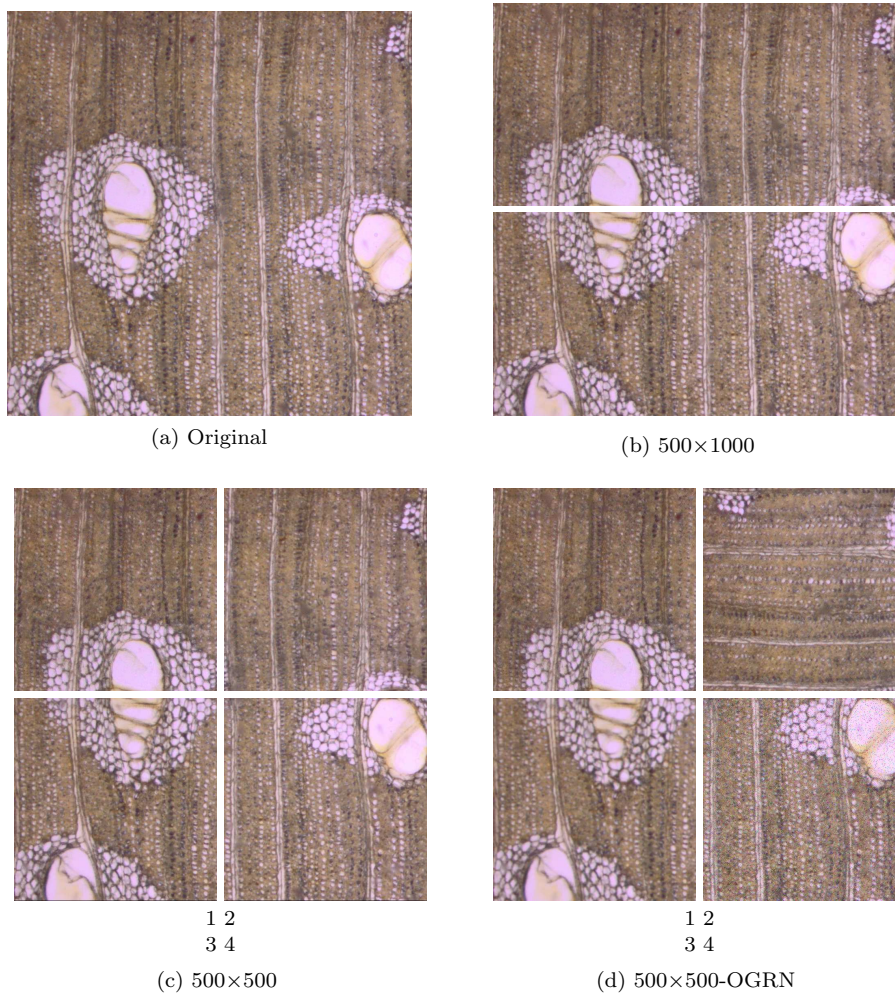
(a) Original

(b) 500×1000

1 2
3 4

(c) 500×500

1 2
3 4

(d) 500×500-OGRN

Fig. 7: Data augmentation procedure. Images from a sample of *Afzelia africana*. (a) Original image. Original image divided in two parts (b) and four parts (c). (d) Original image divided in four parts applying a 2-D Gaussian smoothing kernel with standard deviation of 1 at the second piece, rotating the third piece 90 degrees and adding salt-and-pepper noise with a density of 0.05 to the fourth piece.

5.3 Image preprocessing and feature extraction

To prepare the image data for further analysis, the color images were trans-
formed into grayscale images and digitally enhanced using histogram stretch-
ing (1% saturation tolerance). Subsequently, features were extracted from the
preprocessed images. In this paper, Local Phase Quantization (LPQ) [27,28]
is used as texture feature descriptor, as in most studies involving wood species
identification [18,17,19,21]. In total, 256 LPQ features were used.

5.4 Image classification for species identification

5.4.1 Single-view classification

Most work on the development of machine learning models for the classification
of wood samples based on microscopic imagery relies on a single transversal
image of the sample. For that reason, we use this approach as a baseline. More
precisely, the random forest algorithm [29] was used to construct a classifier
that takes the LPQ features of a transversal image as input and makes a
prediction at species level. The *forest* it builds, is an ensemble of decision trees,
in our case 500 trees. The number of features (randomly) selected at each split
was set to 15. Two additional random forest classifiers were constructed, a
first classifier that takes the LPQ features of the radial image as input and a
second classifier that takes the features of the tangential image as input. All
classifiers were trained independently and evaluated using a cross-validation
scheme (see Section 2).

5.4.2 A multi-view random forest model (MVRF)

The images of the transversal, tangential and radial cross-sections of a wood
sample can be interpreted as multiple views of an object. Several options ex-
ist that allow to incorporate multi-view in a machine learning model. A first
(simple) approach that we explore consists of concatenating the LPQ feature
vectors of the three images. In this case the new feature space is the Carte-
sian product of the three original feature spaces. This approach has at least
three potential downsides: (1) the size of the feature space is tripled in a set-
ting that is already data-scarce; (2) the concatenation is agnostic to the fact
that the features originate from different images and (3) the concatenation is
agnostic to the classification problem at hand. To overcome these problems,
we propose a model architecture that extends the basic random forest model
and allows to combine the multiple views and is inspired on the stacking of
classifiers (see Figure 8 for a visualization of the architecture). In a first step
a separate random forest model is trained for each of the three views using a
training dataset. For each image in the training dataset, the 500 trees in each
random forest then each cast a vote for one of the $q = 77$ classes (the species).
Per image, the relative frequencies of these votes are subsequently combined

into a vector (which is a proxy for the predicted class probabilities). The vectors of the three views that are obtained in this way are then concatenated to form a meta-feature vector. These meta-feature vectors form the inputs of a meta-training dataset (the outputs are the species labels). Subsequently, a multinomial logistic regression model is trained on this meta-dataset to predict the final species label. We conclude this paragraph with a subtle, but important, implementation detail. To obtain the meta-training dataset during training, only out-of-bag votes are used to compute the meta-vector of relative frequencies. Recall that due to the use of bootstrapping, each training observation is used (on average) in only two out of three trees in a forest. As only these trees are allowed to cast a vote, the meta-feature vector will not be prone to overfitting. For allowing this stacking approach to work in practice, the meta-feature vector must be representative for the meta-feature vector of the test instances [30].
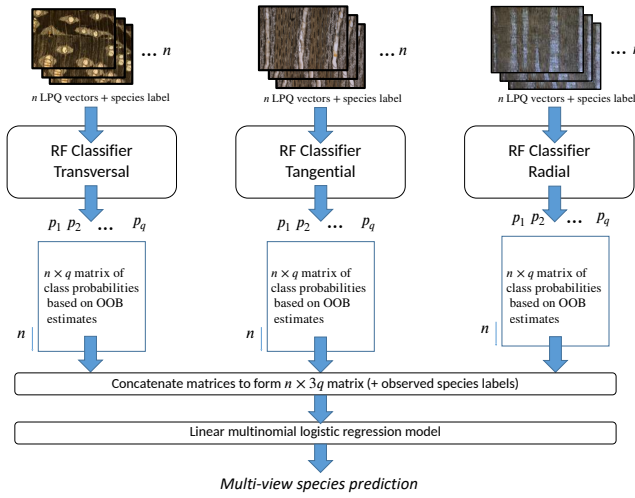

Fig. 8: Visualization of the architecture of the multi-view random forest classifier, where n represents the number of training observations.

5.4.3 Leave-k-trees-out cross-validation

Traditionally, the performance of a classifier is assessed using a separate training set or k-fold cross-validation. The split between test and training set (or the definition of the folds in case of k-fold cross-validation) is made using a (stratified) random sampling scheme, with the aim of constructing a test set that is independent from the training set. However, when working with microscopic imagery of wood samples, and especially those originating from historical collections, a single block of wood is often used to make several

prepared microscopic slides. As a result, the images originate from the same piece of wood and might show less biological variability as compared to images from different pieces of wood. Moreover, they are often made in sequence and therefore under more similar conditions as compared to slides that are prepared during a period spread out in time, possibly by several lab technicians, and so on. As a result, the image-to-image variability within one piece of wood can be assumed to be smaller than the inter-tree variability. As such, when using a stratified cross-validation scheme with stratification at the species level (or stratified train-test split), images of the same piece of wood can end up in both training and test sets. In this way, these sets cannot be considered independent and performance estimates can be too optimistic. As an alternative, we propose a cross-validation scheme which we call 'leave-k-trees-out scheme', in which all images that originate from the same tree are either in the training or the test set. In our results section, we compare a traditional cross-validation scheme (in particular the out-of-bag performance estimator of the random forest classifier, which is almost identical to leave-one-image-out cross-validation [31, 32]) and the leave-k-trees-out scheme.

5.4.4 Including genus and family information in the classification process

In the methods described previously, the accuracy on a test set is used to evaluate the performance of a model. By definition, each misclassified instance has the same influence on the final accuracy. In our (multi-class) species identification problem, it can be argued that this is too simplistic. For example, consider a test instance with true label y and predicted label y'. The case where $y \neq y'$ but both labels belong to the same genus may be not such an issue for some applications than the case where y and y' belong to different genera. Additionally, the cost associated with a misclassification may increase further when y and y' belong to different families. To generalize this example, we define cost functions for which the cost is determined by the genus or family distance between y and y'. We formally define this cost function as follows:

$$
C(y, y') = \begin{cases}
0 & \text{, if } y = y', \\
1 & \text{, if } y \neq y' \text{ and genus}(y) = \text{genus}(y'), \\
1.25 & \text{, if genus}(y) \neq \text{genus}(y') \text{ and family}(y) = \text{family}(y'), \\
1.5 & \text{, otherwise,}
\end{cases}
\tag{1}
$$

where genus(y) and family(y) refer to the genus and the family of y, respectively.

The random forest classifiers, described earlier, are originally designed to optimize accuracy. However, several methods have been described in literature that allow to learn cost-sensitive classifiers [33–35]. Moreover, as the cost function that we use is derived from a tree-like hierarchy on the labels, existing hierarchical classification methods [36] can be used to solve our problem as well. The methods that have been proposed in literature range from simple extensions of traditional learning algorithms, for example relying on over-sampling or threshold moving [37], to more complex dedicated hierarchical classification

algorithms [38]. In this paper, we use an approach that is called a threshold moving algorithm by [37], and essentially is a post-processing of the predicted probability mass function over the classes, to obtain the prediction that minimizes the posterior predictive loss in a Bayesian framework [39].

As a starting point, we refer to $p(y \mid \mathbf{x})$ as the posterior probability that the label, i.e. the species name, of a test instance with a feature vector $\mathbf{x}$ is equal to y. We now select the label y^* that minimizes the expected value of C under the posterior probability mass functions $p(y \mid \mathbf{x})$:

$$y^* = \arg \min_{y' \in Y} \sum_{y \in Y} C(y, y') \, p(y \mid \mathbf{x}) \,, \tag{2}$$

where Y is the label set. During the test phase, $p(y \mid \mathbf{x})$ is not known but is replaced with its estimator, obtained using the random forest classifier. This approach does not require any modification of the random forest learner, as it only relies on a post-processing of the estimated probabilities from a fitted random forest model. When using the random forest classifier in the traditional way, the class with the highest estimated probability is the predicted label. Note that this estimator can still be obtained using the latter strategy by modifying C such that $C(y, y') = 1$ for any $y \neq y'$.

6 Declarations

6.1 Ethics approval and consent to participate

Not applicable

6.2 Consent for publication

Not applicable

6.3 Availability of data and materials

The dataset generated and analysed during the current study is available from the corresponding author on reasonable request.

6.4 Competing interests

The authors declare that they have no competing interests.

6.5 Funding

6.6 Authors' contributions

NRDS contributed to the design and experiments of the work, the interpretation of data and drafted the work; VD analyzed and interpreted the data and results, contributed in writing the manuscript and revised it; JMB substantively contributed to the conception of the work and revised it; JVdB substantively contributed to the conception of the work and revised it; MDR and MR performed the acquisition of data; OMB substantively contributed to the conception of the work and revised it; HB contributed to the acquisition of data, analyzed and interpreted the results and revised the manuscript; JVA substantively contributed to the conception of the work and revised it; BDB substantively contributed to the conception of the work, analysis and substantively revised the manuscript; JV contributed to the conception and design of the work, the interpretation of results, contributed in writing the manuscript and substantively revised it. All authors read and approved the final manuscript.

6.7 Corresponding author

Núbia Rosa da Silva, nubia@ufcat.edu.br, nubiasrosa@gmail.com.

6.8 Acknowledgements

7 Supplementary Materials

7.1 Species, genera and families

Tables 5 and 6 show the species, genera and families of the wood samples used in the experiments.

7.2 2D PCA-plot

Figure 9 shows the 2D PCA-plot of the class *Afzelia africana*. As can be observed, the characteristics of each image continue to be representative and distinct even though the number of samples increases. When the images are divided in two or four parts, the characteristics remain concentrated in the same region. However, when applying the smoothing, noise and rotation operations, the samples tend to spread out, making it difficult to identify them. However, it is important to carry out these operations on the data because they can represent real situations, since the wood samples can be obtained at different times or in adverse situations, and different regions.
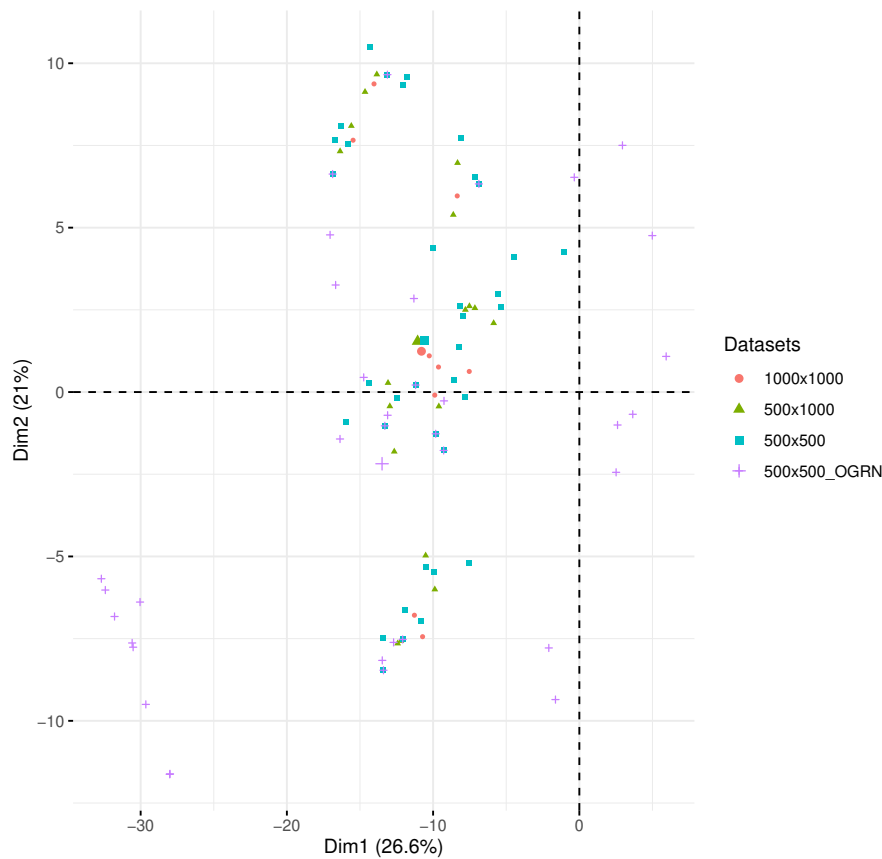

Fig. 9: 2D PCA-plot of the class *Afzelia africana* for the original dataset, the dataset of original images divided in two parts, the dataset of original images divided in four parts and the dataset of original image divided in four parts with noise and rotation.

7.3 Variability of training and testing samples

Figure 10 shows samples of *Lophira alata* species to emphasize the variability between samples from different wood samples.
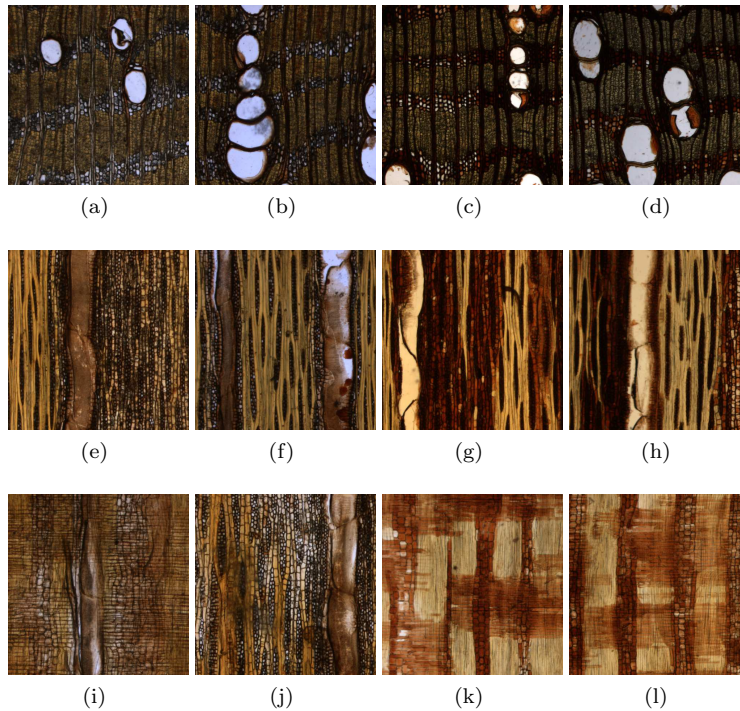

Fig. 10: Samples of *Lophira alata* species. The first and second columns show samples of the training set and the third and fourth columns show samples of the test set for this species. (a)–(d) are transversal, (e)–(h) are tangential and (i)–(l) are radial cross-sections.

References

1. C. May, Transnational crime and the developing world. Tech. rep., Global Financial Integrity (2017)
2. C. Nellemann, *Green Carbon, Black Trade: Illegal Logging, Tax Fraud and Laundering in the World's Tropical Forests. A Rapid Response Assessment. United Nations Environment Programme, GRID Arendal* (United Nations Environment Programme, 2012)
3. U. Nations. Convention on international trade in endangered species of wild fauna and flora. Appendices I, II and III. URL https://cites.org/sites/default/files/eng/disc/CITES-Convention-EN.pdf (accessed October 20, 2021)

4. ITTO, *Biennial review and assessment of the world timber situation* (ITTO Yokohama, Japan, 2016). URL www.ino.int.

5. V. Deklerck, E. Price, S. Vanden Abeele, K. Lievens, E. Espinoza, H. Beeckman, Plant Methods **17**(1), 64 (2021). DOI 10.1186/s13007-021-00766-x. URL https://doi.org/10.1186/s13007-021-00766-x

6. E.R. Price, I.A. Miles-Bunch, P.E. Gasson, C.A. Lancaster, IAWA Journal pp. 1–22 (2021). DOI https://doi.org/10.1163/22941932-bja10064. URL https://brill.com/view/journals/iawa/aop/article-10.1163-22941932-bja10064/article-10.1163-22941932-bja10064.xml

7. F. Ruffinatto, A. Crivellaro, *Atlas of Macroscopic Wood Identification, With a Special Focus on Timbers Used in Europe and CITES-listed Species* (Springer, Cham, 2019). DOI 10.1007/978-3-030-23566-6

8. V. Deklerck, T. Mortier, N. Goeders, R. Cody, W. Waegeman, E. Espinoza, J. Van Acker, J. Van den Bulcke, H. Beeckman, Wood Science and Technology **53**(4), 953 (2019). DOI 10.1007/s00226-019-01111-1

9. J. Braga, T. Pastore, V. Coradin, J. Camargos, A. Silva, IAWA Journal **32**, 285 (2011). DOI 10.1163/22941932-90000058

10. P. Gasson, P. Baas, E. Wheeler, IAWA Journal **32**(2), 155 (2011)

11. S. Hassold, P.P. Lowry, II, M.R. Bauert, A. Razafintsalama, L. Ramamonjisoa, A. Widmer, PLOS ONE **11**(6), 1 (2016). DOI 10.1371/journal.pone.0157881. URL https://doi.org/10.1371/journal.pone.0157881

12. L. Jiao, M. Yu, A.C. Wiedenhoeft, T. He, J. Li, B. Liu, X. Jiang, Y. Yin, Scientific Reports **8**(1), 1945 (2018)

13. T. Pastore, J. Braga, V. Coradin, W. Magalhães, E. Okino, J. Camargos, G. Muniz, O. Bressan, F. Davrieux, Holzforschung **65**, 73 (2011). DOI 10.1515/hf.2011.010

14. E. Wheeler, P. Baas, P. Gasson, IAWA journal / International Association of Wood Anatomists **10**, 219 (1989)

15. E.E. Dormontt, M. Boner, B. Braun, G. Breulmann, B. Degen, E. Espinoza, S. Gardner, P. Guillery, J.C. Hermanson, G. Koch, S.L. Lee, M. Kanashiro, A. Rimbawanto, D. Thomas, A.C. Wiedenhoeft, Y. Yin, J. Zahnen, A.J. Lowe, Biological Conservation **191**, 790 (2015). DOI https://doi.org/10.1016/j.biocon.2015.06.038

16. P. Gasson, IAWA Journal **32**(2), 137 (2011)

17. J. Martins, L.S. Oliveira, S. Nisgoski, R. Sabourin, Machine Vision and Applications **24**(3), 567 (2013)

18. P.L. Filho, L.S. Oliveira, S. Nisgoski, A.S. Britto, Mach. Vision Appl. **25**(4), 1019–1031 (2014). DOI 10.1007/s00138-014-0592-7. URL https://doi.org/10.1007/s00138-014-0592-7

19. N. Rosa da Silva, M. De Ridder, J.M. Baetens, J. Van den Bulcke, M. Rousseau, O. Martinez Bruno, H. Beeckman, J. Van Acker, B. De Baets, Annals of Forest Science **74**(2), 30 (2017). DOI 10.1007/s13595-017-0619-0. URL https://doi.org/10.1007/s13595-017-0619-0

20. P. Ravindran, A. Costa, R. Soares, A.C. Wiedenhoeft, Plant Methods **14**(1), 25 (2018)

21. D. Souza, J. Santos, H. Vieira, T. Naide, S. Nisgoski, L. Soares de Oliveira, Wood Science and Technology (2020). DOI 10.1007/s00226-020-01196-z

22. P. Ravindran, B.J. Thompson, R.K. Soares, A.C. Wiedenhoeft, Frontiers in Plant Science **11**, 1015 (2020). DOI 10.3389/fpls.2020.01015. URL https://www.frontiersin.org/article/10.3389/fpls.2020.01015

23. F. Lens, C. Liang, Y. Guo, X. Tang, M. Jahanbanifard, F.S.C. da Silva, G. Ceccantini, F.J. Verbeek, IAWA Journal **41**(4), 660 (2020). DOI https://doi.org/10.1163/22941932-bja10029

24. A.N. Angelopoulos, S. Bates, arXiv preprint **arXiv:2107.07511** (2021). URL https://arxiv.org/abs/2107.07511

25. A. Muellner, H. Schaefer, R. Lahaye, Molecular Ecology Resources **11**(3), 450 (2011). DOI https://doi.org/10.1111/j.1755-0998.2011.02984.x

26. P. Kitin, E. Espinoza, H. Beeckman, H. Abe, P.J. McClure, Annals of Forest Science **78**(31), 1 (2021). DOI 10.1007/s13595-020-01024-1. URL https://doi.org/10.1007/s13595-020-01024-1

27. V. Ojansivu, J. Heikkilä, in *Image and Signal Processing*, ed. by A. Elmoataz, O. Lezoray, F. Nouboud, D. Mammass (Springer Berlin Heidelberg, Berlin, Heidelberg, 2008), pp. 236–243

28. V. Ojansivu, E. Rahtu, J. Heikkila, in *Pattern Recognition, 2008. ICPR 2008. 19th International Conference on* (2008), pp. 1–4. DOI 10.1109/ICPR.2008.4761377

29. L. Breiman, Machine Learning **45**(1), 5 (2001). DOI 10.1023/A:1010933404324

30. E. Spyromitros-Xioufis, G. Tsoumakas, W. Groves, I. Vlahavas, Machine Learning **104**, 55 (2016). DOI 10.1007/s10994-016-5546-z. URL https://doi.org/10.1007/s10994-016-5546-z

31. L. Breiman, Out-of-bag estimation. Tech. rep., University of California, Berkeley, CA (1996). URL https://www.stat.berkeley.edu/~breiman/OOBestimation.pdf

32. T. Hastie, R. Tibshirani, J. Friedman, *The Elements of Statistical Learning* (Springer-Verlag New York, 2008). DOI 10.1007/978-0-387-84858-7

33. J.P. Dmochowski, P. Sajda, L.C. Parra, Journal of Machine Learning Research **11**, 3313 (2010)

34. P. Domingos, in *Proceedings of the Fifth ACM SIGKDD International Conference on Knowledge Discovery and Data Mining* (Association for Computing Machinery, New York, NY, USA, 1999), KDD'99, pp. 155–164. DOI 10.1145/312129.312220

35. C. Elkan, in *Proceedings of the 17th International Joint Conference on Artificial Intelligence* (Morgan Kaufmann Publishers Inc., San Francisco, CA, USA, 2001), IJCAI'01, p. 973–978

36. C.N. Silla, A.A. Freitas, Data Mining and Knowledge Discovery **22**(1), 31 (2011). DOI 10.1007/s10618-010-0175-9

37. Zhi-Hua Zhou, Xu-Ying Liu, IEEE Transactions on Knowledge and Data Engineering **18**(1), 63 (2006). DOI 10.1109/TKDE.2006.17

38. I. Tsochantaridis, T. Joachims, T. Hofmann, Y. Altun, J. Mach. Learn. Res. **6**, 1453–1484 (2005)

39. C.M. Bishop, *Pattern Recognition and Machine Learning* (Springer, 2006)

Table 5: Species, genera and families.

Species	Genus	Family
Afzelia africana	Afzelia	Fabaceae-Caesalpiniaceae
Afzelia bella	Afzelia	Fabaceae-Caesalpiniaceae
Afzelia bipindensis	Afzelia	Fabaceae-Caesalpiniaceae
Afzelia cuanzensis	Afzelia	Fabaceae-Caesalpiniaceae
Afzelia pachyloba	Afzelia	Fabaceae-Caesalpiniaceae
Albizia adianthifolia	Albizia	Fabaceae-Mimosaceae
Albizia antunesiana	Albizia	Fabaceae-Mimosaceae
Albizia ferruginea	Albizia	Fabaceae-Mimosaceae
Alstonia boonei	Alstonia	Apocynaceae
Amphimas ferrugineus	Amphimas	Fabaceae-Caesalpiniaceae
Amphimas pterocarpoides	Amphimas	Fabaceae-Caesalpiniaceae
Anthonotha macrophylla	Anthonotha	Fabaceae-Caesalpiniaceae
Antiaris toxicaria	Antiaris	Fabaceae-Caesalpiniaceae
Antrocaryon nannanii	Antrocaryon	Anacardiaceae
Autranella congolensis	Autranella	Sapotaceae
Beilschmiedia congolana	Beilschmiedia	Lauraceae
Brachystegia laurentii	Brachystegia	Fabaceae-Caesalpiniaceae
Canarium schweinfurthii	Canarium	Burseraceae
Ceiba pentandra	Ceiba	Bombacaceae
Celtis gomphophylla	Celtis	Ulmaceae
Chrysophyllum africanum	Chrysophyllum	Sapotaceae
Chrysophyllum lacourtianum	Chrysophyllum	Sapotaceae
Copaifera mildbraedii	Copaifera	Fabaceae-Caesalpiniaceae
Cordia platythyrsa	Cordia	Boraginaceae
Cynometra alexandri	Cynometra	Fabaceae-Caesalpiniaceae
Cynometra hankei	Cynometra	Fabaceae-Caesalpiniaceae
Diospyros crassiflora	Diospyros	Ebenaceae
Drypetes gossweileri	Drypetes	Euphorbiaceae
Ekebergia capensis	Ekebergia	Meliaceae
Entandrophragma angolense	Entandrophragma	Meliaceae
Entandrophragma candollei	Entandrophragma	Meliaceae
Entandrophragma cylindricum	Entandrophragma	Meliaceae
Entandrophragma utile	Entandrophragma	Meliaceae
Erythrophleum suaveolens	Erythrophleum	Fabaceae-Caesalpiniaceae
Ficus mucuso	Ficus	Moraceae
Funtumia africana	Funtumia	Apocynaceae
Gilbertiodendron dewevrei	Gilbertiodendron	Fabaceae-Caesalpiniaceae
Guibourtia arnoldiana	Guibourtia	Fabaceae-Caesalpiniaceae
Guibourtia demeusei	Guibourtia	Fabaceae-Caesalpiniaceae
Hallea stipulosa	Hallea	Rubiaceae
Holoptelea grandis	Holoptelea	Ulmaceae
Irvingia grandifolia	Irvingia	Irvingiaceae
Khaya anthotheca	Khaya	Meliaceae
Klainedoxa gabonensis	Klainedoxa	Irvingiaceae
Leplaea cedrata	Leplaea	Meliaceae
Leplaea laurentii	Leplaea	Meliaceae
Leplaea thompsonii	Leplaea	Meliaceae
Lophira alata	Lophira	Ochnaceae
Lovoa trichilioides	Lovoa	Meliaceae
Mammea africana	Mammea	Clusiaceae
Milicia excelsa	Milicia	Moraceae
Millettia laurentii	Millettia	Fabaceae-Papilionaceae
Morus mesozygia	Morus	Moraceae
Musanga cecropioides	Musanga	Moraceae
Nauclea diderrichii	Nauclea	Rubiaceae

Table 6: Species, genera and families. (continued)

Species	Genus	Family
Nesogordonia dewevrei	Nesogordonia	Sterculiaceae
Nesogordonia kabingaensis	Nesogordonia	Sterculiaceae
Newtonia leucocarpa	Newtonia	Fabaceae-Mimosaceae
Ongokea gore	Ongokea	Olacaceae
Pentaclethra eetveldeana	Pentaclethra	Fabaceae-Mimosaceae
Pentaclethra macrophylla	Pentaclethra	Fabaceae-Mimosaceae
Pericopsis elata	Pericopsis	Fabaceae-Papilionaceae
Petersianthus macrocarpus	Petersianthus	Lecythidaceae
Piptadeniastrum africanum	Piptadeniastrum	Fabaceae-Mimosaceae
Pouteria aningeri	Pouteria	Sapotaceae
Prioria balsamifera	Prioria	Fabaceae-Caesalpiniaceae
Prioria oxyphylla	Prioria	Fabaceae-Caesalpiniaceae
Pterocarpus soyauxii	Pterocarpus	Fabaceae-Papilionaceae
Pterocarpus tinctorius	Pterocarpus	Fabaceae-Papilionaceae
Pycnanthus angolensis	Pycnanthus	Myristicaceae
Scorodophleus zenkeri	Scorodophloeus	Fabaceae-Caesalpiniaceae
Staudtia kamerunensis	Staudtia	Myristicaceae
Terminalia superba	Terminalia	Combretaceae
Tessmannia africana	Tessmania	Fabaceae-Caesalpiniaceae
Tieghemella heckelii	Tieghemella	Sapotaceae
Triplochiton scleroxylon	Triplochiton	Sterculiaceae
Zanthoxylum gilletii	Zanthoxylum	Rutaceae
Zanthoxylum lemairei	Zanthoxylum	Rutaceae